NF-κB Functions in Stromal Fibroblasts to Regulate Early Postnatal Muscle Development*[S]

Jason M. Dahlman[‡§], **Nadine Bakkar**[‡], **Wei He**[‡¶], **and Denis C. Guttridge**[‡§¶‖1]

From the ‡Department of Molecular Virology, Immunology, and Medical Genetics, Human Cancer Genetics Program, the §Integrated Biomedical Sciences Graduate Program, the ¶Molecular, Cellular, and Developmental Biology Graduate Program, and the ‖Arthur G. James Comprehensive Cancer Center, The Ohio State University, Columbus, Ohio 43210

Classical NF-κB activity functions as an inhibitor of the skeletal muscle myogenic program. Recent findings reveal that even in newborn *RelA/p65⁻/⁻* mice, myofiber numbers are increased over that of wild type mice, suggesting that NF-κB may be a contributing factor in early postnatal skeletal muscle development. Here we show that in addition to p65 deficiency, repression of NF-κB with the IκBα-SR transdominant inhibitor or with muscle-specific deletion of IKKβ resulted in similar increases in total fiber numbers as well as an up-regulation of myogenic gene products. Upon further characterization of early postnatal muscle, we observed that NF-κB activity progressively declines within the first few weeks of development. At birth, the majority of this activity is compartmentalized to muscle fibers, but by neonatal day 8 NF-κB activity from the myofibers diminishes, and instead, stromal fibroblasts become the main cellular compartment within the muscle that contains active NF-κB. We find that NF-κB functions in these fibroblasts to regulate inducible nitric-oxide synthase expression, which we show is important for myoblast fusion during the growth and maturation process of skeletal muscle. Together, these data broaden our understanding of NF-κB during development by showing that in addition to its role as a negative regulator of myogenesis, NF-κB also regulates nitric-oxide synthase expression within stromal fibroblasts to stimulate myoblast fusion and muscle hypertrophy.

NF-κB belongs to a family of transcription factors that contains five subunits: RelA/p65, c-Rel, RelB, p50, and p52 (1–3). These members are characterized by a highly conserved 300-amino acid N-terminal Rel domain that mediates subunit dimerization, DNA binding, and interaction with the NF-κB inhibitor proteins (IκBs)[2] (4, 5). RelA/p65 (referred to as p65

from here on), c-Rel, and RelB also contain C-terminal transactivation domains that are necessary for the initiation of NF-κB-dependent transcription (4, 5). The p50 and p52 subunits are processed forms of the IκB proteins p105 and p100, respectively (1–3), and because these mature proteins lack an activation domain, they undergo dimerization with p65, c-Rel, or RelB to form transcriptionally active complexes (2, 6).

Classical NF-κB activity is initiated in response to extracellular signals such as inflammatory cytokines, which trigger the activation of the IκB kinase (IKK) complex composed of two catalytic subunits, IKKα and IKKβ, and a regulatory subunit, IKKγ or NEMO (2, 7). The activated IKK complex, via IKKβ, phosphorylates IκB bound to NF-κB, which leads to IκB ubiquitination and subsequent proteasomal degradation. Released NF-κB, most commonly found as a p65/p50 heterodimer, is then free to translocate to the nucleus, where it binds and regulates the expression of its target genes (8, 9).

NF-κB regulates a number of cellular processes including immune response, cell survival, and proliferation. Additionally, NF-κB is also considered an important player in tissue differentiation including skin (10), bone (11), and skeletal muscle (12). With respect to muscle, this differentiation program is regulated in large part by Pax3 and Pax7 transcription factors, whose expression undergo down-regulation within proliferating muscle progenitor cells to allow the initiation of myogenesis (13, 14). This is followed by the activation and induction of skeletal muscle-specific transcription factors, MyoD, Myf-5, myogenin, and MRF4, which govern key myogenic processes such as cell cycle exit, myoblast fusion, and contractile function (15–17).

Although the role of NF-κB in skeletal muscle differentiation is still evolving, recent genetic findings implicate this signaling pathway as an inhibitor of myogenesis. Early studies showed that myogenesis in cultured cell lines was associated with declining activity of the classical NF-κB subunits (18), and TNFα was capable of suppressing MyoD expression and inhibiting myogenesis through the activation of p65 (19, 20). NF-κB was also found to repress muscle differentiation through the induction of YY1, which in association with Polycomb proteins silences myofibrillar genes as well as the pro-myogenic microRNA, miR-29 (21–23). Recent genetic analysis performed in primary muscle cells and injured adult skeletal muscles from p65 and IKKβ mutant mice further supports the role of NF-κB as an inhibitor of myogenesis (24–26).

Consistent with the findings above, analysis of muscles from newborn *p65⁻/⁻* mice (which were maintained on a *TNFα⁻/⁻*

background to circumvent p65 null lethality and from here on referred to only as $p65^{-/-}$ mice) (27) revealed a significant increase in the total number of myofibers (25). This phenotype suggested that the inhibitory myogenic activity of NF-κB is present in the early phases of postnatal muscle development. In the process of attempting to better characterize NF-κB during this stage of muscle maturation, we observed NF-κB activation in the stromal compartment specific to fibroblasts. In the following study we describe the ability of these stromal fibroblasts to regulate inducible nitric-oxide synthase (iNOS) expression in an NF-κB-dependent manner, which functions to promote myoblast fusion and in turn ensures proper skeletal muscle growth.

EXPERIMENTAL PROCEDURES

Materials—Cell Tracker Orange (5-(and-6)-(4-chloromethylbenzoylamino)tetramethylrhodamine (CMTMR)), cytomegalovirus-iNOS, Moloney murine leukemia virus, reverse transcriptase, Trizol reagent, Fungizone, Dulbecco's modified Eagle's medium, F-10 media, penicillin/streptomycin, and protease inhibitors were obtained from Invitrogen. DAPI mounting gel was acquired from Electron Microscopy Sciences (Hatfield, PA). Collagenase type I and insulin were purchased from Sigma. Falcon Filters were acquired from BD Biosciences. Collagenase type II was obtained from Worthington Biochemical (Lakewood, NJ). Control and iNOS-targeted siRNA was obtained from Dharmacon (Lafayette, CO). Collagenase P was purchased from Roche Applied Science. Mammalian protein extraction reagent (MPER) was acquired from Thermo Scientific (Rockford, IL). Homogenizing buffer for skeletal muscle homogenization was prepared with the following composition: 1% Triton X, 150 mM NaCl, 50 mM Tris-HCl, 1 mM EDTA, 1 mM phenylmethylsulfonyl fluoride, 5 μl/ml protease inhibitors (Sigma). Primers for PCR reactions were obtained from DNA Primer Solutions and are listed in supplemental Table 1.

Antibodies—Antibodies against IκBα, p100, p50, MyoD, vimentin, and glyceraldehyde-3-phosphate dehydrogenase were obtained from Santa Cruz Biotechnology (Santa Cruz, CA); ER-TR7 and fibroblast-activating protein were from AbCam (Cambridge, MA); α-tubulin, laminin, and myosin heavy chain (MyHC) were from Sigma; Pax7 was from The Developmental Studies Hybridoma Bank (Iowa City, IA); iNOS was from BD Biosciences; phosphorylated-IκBα, phosphorylated p65 (p-p65; Ser-536), and phosphorylated IκBα (p-IκBα; Ser-32) were from Cell Signaling (Boston, MA); p65 was from Rockland Immunochemical Inc. (Gilbertsville, PA); dystrophin was from Novocastra Laboratories Ltd. (Newcastle, UK); CD31 was from BD Pharmingen; CD68 was from AbD Serotec (Raleigh, NC); GFP and Alexa Fluor secondary antibodies were from Invitrogen (Carlsbad, CA).

Mice—Animals were housed in the animal facility at The Ohio State University Comprehensive Cancer Center under sterile conditions with temperature and humidity kept constant and fed a standard diet. Treatment of the mice was in accordance with institutional guidelines of the Animal Care and Usage Committee. $p65^{-/-}$, $p65^{-/-}$;TNF-$\alpha^{-/-}$, $IKK\beta^{f/f}$, NF-κB$^{+/EGFP}$, and collagen type 1a YFP mice were generated as previously described (27–31). $iNOS^{-/-}$ and wild type CD2 and C57BL/6

mice were purchased from The Jackson Laboratory (Bar Harbor, ME).

Cell Culture—C2C12 myoblasts, mouse embryonic fibroblasts (MEFs), and primary myoblasts were cultured as previously described (25). Primary fibroblasts were isolated according to the myoblast purification pre-plating steps as described by Rando and Blau (32). Primary fibroblasts were cultured in complete Dulbecco's modified Eagle's medium (20% fetal bovine serum, 2% penicillin/streptomycin).

Transient Transfections and Virus Infection—For knockdown studies, MEFs were transfected with control or iNOS siRNA from Dharmacon (in low-serum Opti-MEM using Lipo2000 reagent from Invitrogen), according to the manufacturer's recommendations. For overexpression experiments, MEFs were transfected with control or iNOS cytomegalovirus expression plasmids in serum free Dulbecco's modified Eagle's medium using Superfect reagent from Qiagen (Valencia, CA). Adenovirus-GFP (Ad-GFP) and adenovirus-IκBα super-repressor (Ad-IκBα-SR) viruses were obtained from the University of North Carolina Vector Core facility (Chapel Hill, NC). For *in vivo* infection, 3-day-old neonates were injected in the left hind limb with 1×10^{11} virus particles. Injected mice were euthanized at 8 days of age, and histological analysis of the soleus muscle was performed.

Immunohistochemical Staining—Frozen tissue sections were prepared as previously described (25) and immunostained with the following antibodies and dilutions: GFP (1:500), dystrophin (1:300), Pax7 (1:100), MyoD (1:50), vimentin (1:200), ER-TR7 (1:200), laminin (1:500), MyHC (1:500), CD31 (1:500), CD68 (1:500), and phosphorylated p65 (1:500). For indirect immunofluorescence analysis, Alexa Fluor rhodamine and fluorescein isothiocyanate-conjugated secondary antibodies (1:250) were used. For immunohistochemical staining, a biotinylated secondary antibody was used, and reactions were developed using avidin-biotin complexed with peroxidase.

Histological Analysis—For 8-day-old neonates, whole hind limbs were sectioned at 10 μm with a cryostat (Leica 1900) and stained with hematoxylin and eosin. Specimens were collected after 1000 μm was removed from the proximal end of the hind limb. The total number of muscle fibers within the soleus was determined by sectioning an additional 1600 μm of tissue into the hind limb and averaging the total number of fibers every 200 μm. For sublaminar nuclei determination, tibialis anterior (TA) muscles from 4-week-old mice were sectioned at 10 μm. Specimens were collected after 500 μm was removed from the proximal end of the TA. Sections were then immunostained with laminin and DAPI. Nuclei per fiber counts were then quantitated by determining the number of sublaminar nuclei from 10 randomly chosen fields from 3 littermate pairs of mice.

Electrophoretic Mobility Shift Assays—Nuclear extracts were prepared from skeletal muscles, and electrophoretic mobility shift assays were performed as previously described (33). For supershift assays, nuclear extracts were preincubated for 10 min with 1.5 μg of antibody before the addition of ^{32}P-labeled oligonucleotide probe.

Immunoblotting—Whole cell lysates were prepared from neonatal skeletal muscle, cultured cells, and FACS-sorted GFP$^+$ and GFP$^-$ cells using previously described methods (24).
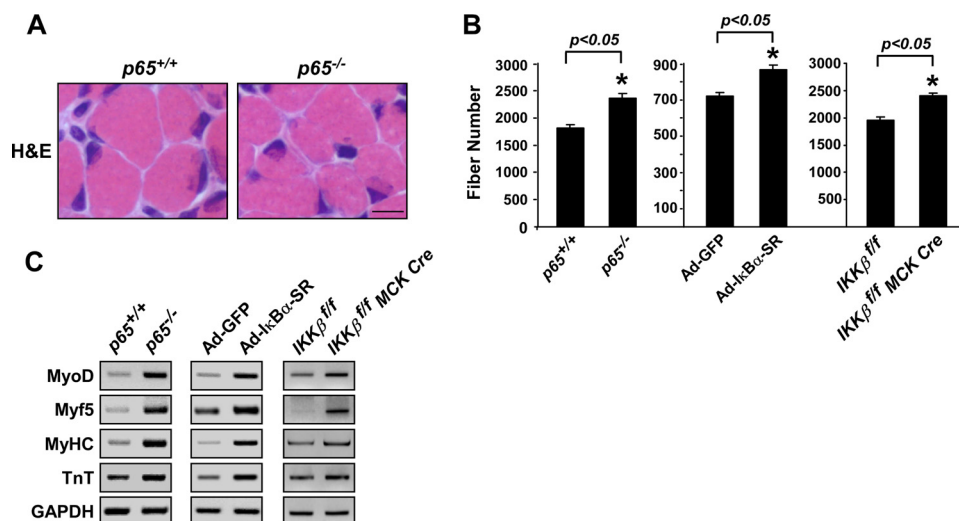
FIGURE 1. **Classical NF-κB signaling functions as a myogenic inhibitor during postnatal muscle development.** *A*, cross-sections of P8 hind limbs from *p65*^{+/+};*TNF*^{−/−} (*p65*^{+/+}) and *p65*^{−/−};*TNF*^{−/−} (*p65*^{−/−}) mice were stained with hematoxylin and eosin (*H&E*). *Scale bar* = 10 μm. *B*, soleus muscle fiber counts were performed on hind limb cross-sections of P8 *p65*^{+/+} and *p65*^{−/−}, Ad-GFP and Ad-IκBα-SR, and *IKKβ*[f/f] and *IKKβ*[f/f] *MCK-CRE* mice (*n* = 3) as described under "Experimental Procedures." *C*, mRNA was isolated from the skeletal muscles of *p65*^{+/+} and *p65*^{−/−}, Ad-GFP and Ad-IκBα-SR, and *IKKβ*[f/f] and *IKKβ*[f/f] *MCK-CRE* mice, and expression of myogenic markers, MyoD, Myf5, MyHC, and troponin (*TNT*) were visualized by semiquantitative PCR. *GAPDH*, glyceraldehyde-3-phosphate dehydrogenase.

Mononuclear Cell Preparation—Hind and fore limbs from 8-day-old NF-κB[+/EGFP] and collagen type 1a YFP mice were digested with 4 ml of 5 mg/ml collagenase type II in a 35-mm polystyrene dish at 37 °C. Digesting limbs were triturated every 10 min with a 5-ml pipette for half an hour. At the end of the digestion 4 ml of digested solution and 6 ml of complete Dulbecco's modified Eagle's medium (2% fetal bovine serum, 1% 1 M HEPES) were transferred to a 15-ml falcon tube to stop the enzymatic reaction. The digested solution was passed through a 70-μm falcon filter and centrifuged for 10 min at 1500 rpm at 4 °C. The supernatant was removed, and the pellet was resuspended in 5 ml of ice-cold phosphate-buffered saline containing 0.5% bovine serum albumin. The resuspended sample was then overlaid with 7 ml of heat-inactivated horse serum and centrifuged for 10 min at 220 × *g* at 4 °C with no brakes. The supernatant was once again removed, and the pellet was resuspended in 5 ml of ice-cold phosphate-buffered saline containing 0.5% bovine serum albumin and centrifuged for 10 min at 1500 rpm at 4 °C. Cell pellets were then resuspended in 1 ml of ice-cold phosphate-buffered saline containing 0.5% bovine serum albumin. Fluorescence-activated cell sorting (FACS) (BD Aria, BD Biosciences) was utilized to isolate GFP[+] and GFP[−] cellular populations.

Single Myofiber Isolation and Staining—Individual muscle fibers were isolated as previously described (34). In short, gastrocnemius muscles were procured from 4-week-old mice and digested in a 35-mm polystyrene dish in 0.2% collagenase type I at 37 °C. Every 15 min the 35-mm polystyrene dishes were shaken by hand until individual muscle fibers were loosened from the muscle bulk. Individual fibers were isolated by triturating the muscle bulk and subsequently transferred to Matrigel-coated polystyrene dishes. Myofibers were then incubated at 37 °C for 30 min and centrifuged for 20 min at 3000 rpm. Myofibers were fixed in 4% paraformaldehyde followed by paraformaldehyde quenching in 100 mM glycine (0.75 g glycine, 2 ml of 10% Triton X-100, and 1 ml 10% sodium azide in 100 ml of H_2O). Single fibers were then blocked, mounted with a DAPI-containing antifade reagent, and placed under a coverslip. Fiber quantitation was performed by scoring the total number of nuclei residing within a single fiber from 20 individual fibers imaged by fluorescent and phase microscopy.

Co-culture Analysis—Isolated primary fibroblasts were stained with 20 μM Cell Tracker Orange CMTMR for 30 min at 37 °C. Stained primary fibroblasts along with unstained C2C12 myoblasts were then trypsinized and counted using a hemocytometer. 1×10^4 primary fibroblasts were co-cultured with 1×10^5 C2C12 myoblasts in fibroblast culture media for 24 h in 35-mm polystyrene dishes. After 24 h, co-cultured cells were switched to differentiation media for 3 days after which they were fixed in 4% paraformaldehyde for 30 min and stained with MyHC and DAPI. Quantitation of myoblast fusion was performed by determining the average number of nuclei per C2C12 myotube from 10 randomly selected fields performed from two independent experiments.

Statistical Analysis—All quantitative data are represented as the means ± S.E. Analysis was performed between different groups using a two-tailed *t* test. Statistical significance was set at $p < 0.05$.

RESULTS

NF-κB Regulates Myogenesis during Early Postnatal Development—Given that deletion of NF-κB signaling was found to impact myogenesis in adult mice (24–26, 35) and that this phenotype could be replicated in newborn animals (25), we sought to more closely examine the role of NF-κB in early postnatal muscle growth. Similar to previous findings (25), we observed that muscles from *p65*^{−/−} neonatal mice at 8 days of age (P8) exhibited a significant increase in total myofiber number (Fig. 1, *A* and *B*). Likewise, *p65*^{−/−} muscles during early postnatal development expressed higher levels of early and late myogenic markers (Fig. 1*C*). However, no such changes were found in the expression of established mediators of muscle development such as myostatin or Notch-1 (36–38) (supplemental Fig. 1, *A* and *B*), suggesting that these effects were specific to NF-κB. To test the validity of our findings, hind limb muscles of P3 wild type mice were infected with adenovirus expressing the IκBα-SR (Ad-IκBα-SR) inhibitor of NF-κB. Compared with injected Ad-GFP controls, muscles expressing the IκBα-SR transgene (supplemental Fig. 2*A*) promoted a similar increase in total fiber number and expression of myogenic gene products as seen in *p65*^{−/−} neonatal mice (Fig. 1, *B* and *C*).
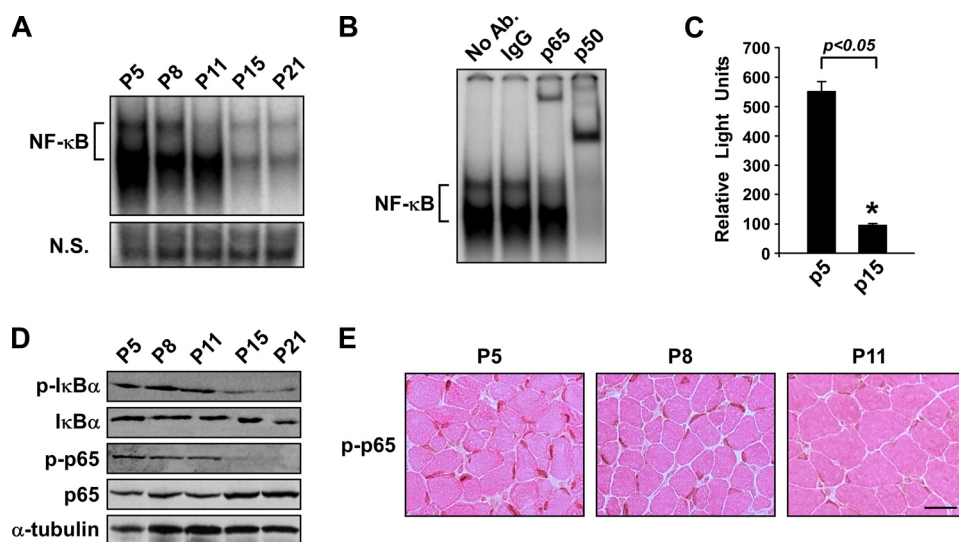
FIGURE 2. **Classical NF-κB signaling activity is reduced during early postnatal skeletal muscle development.** *A*, electrophoretic mobility shift assay analysis was performed on nuclear extracts isolated from the skeletal muscles of P5-P21 wild type mice. Equal loading of nuclear extracts was compared with a nonspecific band on the same gel (*N.S.*). *B*, electrophoretic mobility shift assay super shift analysis was performed on P5 nuclear extracts from *A* with antibodies raised against the p65 and p50 subunits. *Ab*, antibody. *C*, whole cell extracts were isolated from the skeletal muscles of P5 and P15 NF-κB reporter mice (3xκB-Luc-Tg mice) and subjected to luciferase assay analysis. *D* and *E*, whole cell lysates were prepared from wild type P5-P21 skeletal muscle in homogenizing buffer followed by Western blot analysis for p-IκBα and p-p65 (*D*) as well as immunohistochemical staining for p-p65 on wild type P5-P11 hind limb cross-sections (*E*). Eosin was used as a counterstain as shown in *E*. Scale bar = 20 μm.
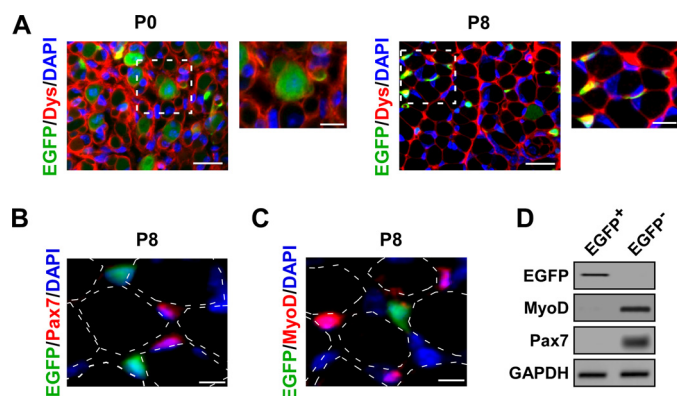

FIGURE 3. **NF-κB activity switches cellular compartments during postnatal skeletal muscle development.** *A*, immunofluorescent staining for dystrophin (*Dys; red*) was performed on hind limb cross-sections of P0 and P8 NF-κB$^{+/EGFP}$ (EGFP; *green*) mice. Areas shown as *dashed boxes* represent fields magnified at 2×. *Scale bars* = 20 and 10 μm, respectively. *B* and *C*, P8 NF-κB$^{+/EGFP}$ (EGFP; *green*) hind limb muscle cross-sections were immunostained with Pax7 (*red, B*) or MyoD (*red, C*). *Dotted outlines* denote the relative position of myofibers that were identified by the overexposure of fluorescent and phase contrast imaging. *Scale bar* = 5 μm. *D*, mononuclear cells were prepared from P8 NF-κB$^{+/EGFP}$ mice. EGFP$^+$ and EGFP$^-$ cells were isolated by FACS sorting and further probed by semiquantitative PCR for EGFP, MyoD, and Pax7. *GAPDH*, glyceraldehyde-3-phosphate dehydrogenase.

This effect was specific to NF-κB as IκBα-SR-expressing muscles displayed lower levels of NF-κB transcriptional activity (supplemental Fig. 2*B*) as measured by NF-κB reporter mice (3xκB-Luc-Tg) (29). Myofiber counts were also performed in muscles from young mice conditionally lacking IKKβ (24–26). Results showed that *IKKβ$^{f/f}$ MCK-CRE* muscles contained a similar increase in fibers and higher expression of myogenic markers as compared with controls (Fig. 1, *B* and *C*). Taken together, these data corroborate findings from adult muscles

demonstrating that NF-κB functions as a potent regulator of skeletal myogenesis even in the early phases of postnatal muscle growth.

NF-κB Signaling Is Active during Early Postnatal Muscle Development—In line with the functional relevance of NF-κB during early postnatal muscle development, we observed that NF-κB activity in whole muscles undergoes dramatic changes within the first 3 weeks of life. By electrophoretic mobility shift assay analysis, NF-κB DNA binding activity was found to be relatively high in newborn mice (P5), and this activity remained elevated for nearly 2 weeks before rapidly declining (Fig. 2*A*). Supershift analysis identified p65 and p50 as the predominant subunits contributing to NF-κB binding activity (Fig. 2*B*). A similar regulatory pattern was observed in muscles from 3xκB-Luc-Tg mice, demonstrating that NF-κB transcriptional activity is initially high but then decreases during this same 2-week developmental window (Fig. 2*C*). Western and immunohistochemical analysis further revealed that this decrease in NF-κB activity was associated with the loss of p-IκBα and p-p65 expression (Fig. 2, *D* and *E*). Because IκBα and p65 (Ser-536) are both phosphorylated by IKKβ (39–42), these results suggest that the regulation of NF-κB in postnatal muscle development occurs through the classical pathway.

NF-κB Is Activated in Stromal Fibroblasts of Postnatal Skeletal Muscle—To better understand how NF-κB regulates muscle development during this early stage of postnatal growth, we sought to identify the cellular compartments responsible for this activity. For this analysis, we utilized EGFP reporter mice under the control of an NF-κB-driven promoter (NF-κB$^{+/EGFP}$) (29). Hind limb muscle cross-sections from P0 and P8 mice were examined for EGFP expression and co-stained with dystrophin to identify myofiber boundaries. Interestingly, at birth and shortly afterward, the majority of NF-κB activity was localized to muscle fibers, but by P8 this activity switched from myofibers to cells in the interstitial space (Fig. 3*A*).

To determine whether NF-κB activity within the interstitium derived from progenitor muscle cells or migrating myoblasts, we imaged EGFP-expressing cells and performed immunostaining with defined myogenic cellular markers. Results showed that in P8 muscles EGFP failed to co-localize with Pax7$^+$ muscle progenitor cells (Fig. 3*B*) or with MyoD$^+$-expressing myoblasts (Fig. 3*C*). To verify that this regulation was not due to potential artifacts of the EGFP reporter system, P8 wild type muscle cross-sections were immunostained with p-p65 and either Pax7 or MyoD. Similar to the reporter signal, p-p65 activity did not cross-react with Pax7$^+$ or MyoD$^+$ cells (supplemental Fig. 3, *A* and *B*), suggesting that muscle progen-
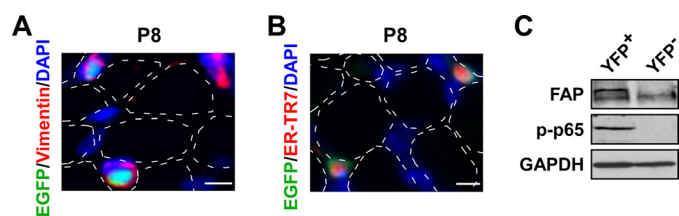
FIGURE 4. **NF-κB is activated in the stromal fibroblasts of postnatal skeletal muscle.** *A* and *B*, immunofluorescent staining was performed on P8 NF-κB$^{+/EGFP}$ (EGFP; *green*) hind limb muscle cross-sections with the mesenchymal marker vimentin (*red*; *A*) and the fibroblast-specific marker ER-TR7 (*red*; *B*). Similar to Fig. 3, the *dotted outlines* indicate the relative position of myofibers. *Scale bar* = 5 μm. *C*, YFP$^+$ and YFP$^-$ mononuclear cells were isolated from P8 collagen type 1a YFP transgenic mice and FACS sorted. Whole cell lysates were prepared from these individual cellular populations and Western blots were performed probing for p-p65 and fibroblast-activating protein (*FAP*). *GAPDH*, glyceraldehyde-3-phosphate dehydrogenase.

itors and myoblasts are not the source of NF-κB activity during this stage of muscle maturation. To confirm our findings, mononuclear cells were prepared from the skeletal muscles of P8 NF-κB$^{+/EGFP}$ mice, and both EGFP$^+$ and EGFP$^-$ cellular populations were subsequently separated by FACS sorting (supplemental Fig. 3C). In line with immunostaining results, MyoD and Pax7 expression was restricted to the EGFP$^-$ population, whose purity was further substantiated by probing for EGFP (Fig. 3D).

To identify the cellular origin of NF-κB activity in neonatal muscles, we screened for markers of various cell types known to reside in the muscle interstitial space, such as endothelial (CD31), myeloid (CD68), and mesenchymal (vimentin). Of these, only vimentin co-localized with EGFP (Fig. 4A and data not shown). Because vimentin cross-reacts with fibroblasts (43), we stained P8 muscles with ER-TR7, a reticular fibroblast marker. Our findings revealed that ER-TR7 did in fact co-localize with EGFP (Fig. 4B), suggesting that NF-κB activity derives from stromal fibroblasts in developing postnatal skeletal muscle. To confirm this notion, we screened for NF-κB activity in muscles from reporter mice containing YFP under the control of the collagen type 1a promoter, which is activated in fibroblasts (31). Preparation of mononuclear cells from these mice at P8 and subsequent FACS sorting validated that NF-κB activity, as measured by p-p65 protein, was indeed present in collagen 1a driving YFP$^+$ cells (Fig. 4C). In addition, the fibroblast activating protein marker was also restricted to the YFP$^+$ cells, demonstrating the purity of the YFP reporter system. Together, these data reveal the novel finding that NF-κB is active in skeletal muscle stromal fibroblasts during early postnatal muscle development.

NF-κB Regulates iNOS Expression within Stromal Fibroblasts of Young Postnatal Muscle—To determine the significance of NF-κB activity within stromal fibroblasts during this stage of development, we assessed potential signaling mediators that might emanate from fibroblasts and could be under the control of NF-κB. On our list we considered fibroblast growth factor-1 and -6 and TGF-β because these genes all contained reported or predicted NF-κB consensus sites in their promoters and, in addition, are known inhibitors of myoblast differentiation (44–46). We also chose to examine inducible iNOS because this gene is an established transcriptional target of NF-κB, which regulates myoblast fusion through the generation of nitric
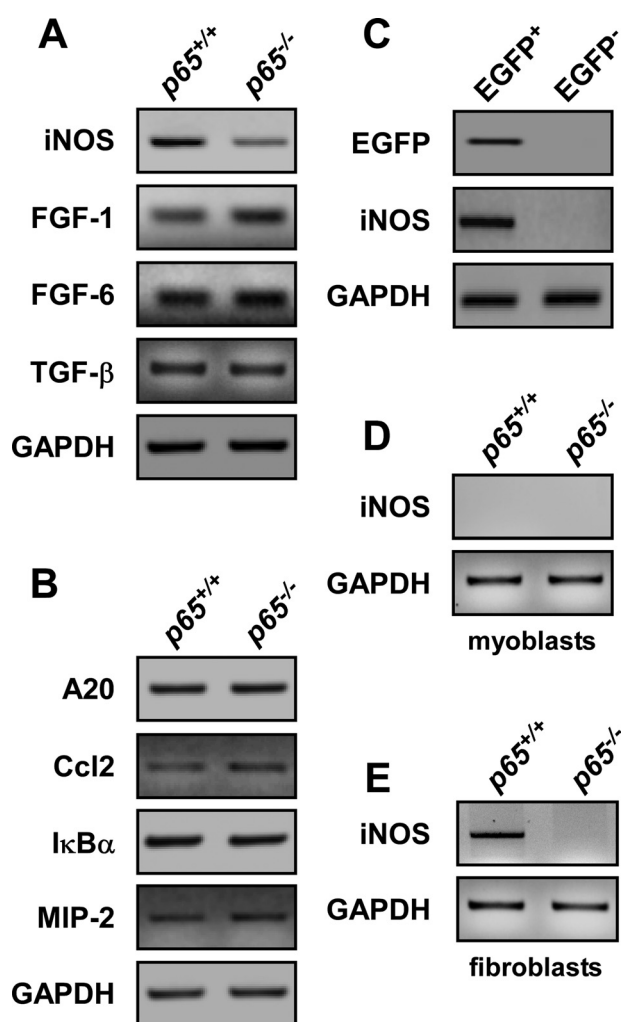

FIGURE 5. **NF-κB regulates iNOS expression in stromal fibroblasts during postnatal muscle development.** *A* and *B*, mRNA was isolated from the skeletal muscles of P8 *p65$^{+/+}$* and *p65$^{-/-}$* mice and the expression of iNOS, fibroblast growth factor-1 and -6, and TGF-β (*A*) as well as other (*B*) established NF-κB-regulated genes was examined by semiquantitative PCR. *C*, EGFP$^+$ and EGFP$^-$ mononuclear cells were sorted from NF-κB$^{+/EGFP}$ mice and probed for iNOS expression by semiquantitative PCR. *D* and *E*, primary myoblasts and fibroblasts were isolated from *p65$^{+/+}$* and *p65$^{-/-}$* mice and iNOS expression was determined by semiquantitative PCR. *GAPDH*, glyceraldehyde-3-phosphate dehydrogenase.

oxide (NO) (47–50). Of these, only iNOS was significantly down-regulated in *p65$^{-/-}$* muscles compared with wild type (Fig. 5A). This regulation appeared specific to iNOS as loss of p65 did not have a general effect on other established NF-κB-dependent genes, such as A20, Ccl2, IκBα, or MIP-2 (Fig. 5B).

In an effort to determine whether iNOS was located within the stromal fibroblast population identified to contain active NF-κB, we examined iNOS expression in P8 FACS-sorted cells isolated from NF-κB$^{+/EGFP}$ mice. PCR analysis detected a strong iNOS signal in the EGFP$^+$ cellular population (Fig. 5C). To further address this point, primary myoblast and fibroblast cultures were prepared from P8 *p65$^{+/+}$* and *p65$^{-/-}$* muscles using routine pre-plating techniques that are employed during standard myoblast isolation (32). The purity of these individual cultures was confirmed by cell type-specific immunostaining and morphological analysis (data not shown). Results showed that iNOS was not expressed in proliferating myoblasts,

whereas its expression was readily detectable in $p65^{+/+}$, but not $p65^{-/-}$ fibroblasts (Fig. 5, *D* and *E*). These data demonstrate that NF-κB activity in stromal fibroblasts functions to regulate

FIGURE 6. Loss of p65 leads to a decrease in myofiber nucleation. *A* and *B*, TA muscles from 4-week-old $p65^{+/+}$ and $p65^{-/-}$ mice ($n = 3$) were sectioned and stained with laminin and DAPI. Histological analysis was subsequently performed to quantitate sublaminar nuclei per fiber numbers. *Scale bar* = 10 μm. *C* and *D*, single fibers were isolated from the gastrocnemius muscles of 4-week-old $p65^{+/+}$ and $p65^{-/-}$ mice and then stained with DAPI to analyze the total number of nuclei per fiber by fluorescent and phase contrast microscopy. *Scale bar* = 20 μm. Quantitation for *B* and *D* was performed as described under "Experimental Procedures."

iNOS expression during a defined developmental window of postnatal skeletal muscle development.

iNOS Regulation by NF-κB Is Important for Myoblast Fusion in Postnatal Muscle—In keeping with published reports suggesting that NO functions to regulate myoblast fusion in culture (48, 49), we examined whether there was a fusion defect associated with p65-deficient muscles. Scoring for sublaminar myonuclei in TA muscles from 4-week-old $p65^{+/+}$ and $p65^{-/-}$ mice revealed a pronounced 43% decrease in the average number of nuclei per fiber in the absence of p65 (Fig. 6, *A* and *B*). Likewise, a 48% reduction in nuclei was measured from individual muscle fibers isolated from gastrocnemius muscles of aged-matched $p65^{+/+}$ and $p65^{-/-}$ mice (Fig. 6, *C* and *D*), suggesting that global deletion of p65 contributes to a fusion defect associated with skeletal muscle maturation.

To determine whether NF-κB activity derived from fibroblasts could regulate myoblast fusion in maturing muscles, purified $p65^{+/+}$ and $p65^{-/-}$ fibroblasts were isolated from P8 muscles, stained with a cell tracker dye (CMTMR orange), and co-cultured at a ratio of 1:10 with C2C12 myoblasts. When co-cultures were switched to differentiation conditions to induce C2C12 myogenesis, we measured a marked 26% reduction in myotube nucleation from cultures containing $p65^{-/-}$ fibroblasts compared with wild type cells (Fig. 7, *A* and *B*). Further analysis revealed that co-cultures containing $p65^{-/-}$ fibroblasts exhibited a 51% decrease in the number of C2C12 myotubes containing 4 or more nuclei per fiber (data not shown).

In contrast to previous findings where we demonstrated that the absence of p65 in primary myoblasts or silencing of p65 by siRNA in C2C12 myoblasts caused myotube formation to be enhanced (25), here in this co-culture system the total number of myotubes remained the same (supplemental Fig. 4), arguing that fibroblast-derived NF-κB activity is responsible for regulating myoblast fusion but is not involved in controlling myogenesis.

Based on these results, we further investigated whether iNOS expression within the fibroblast cellular compartment was a key component in this fusion process by transfecting wild type MEFs with control or iNOS siRNA. RNA and protein analysis confirmed that iNOS was efficiently silenced (supplemental Fig. 5, *A* and *B*). siRNA-targeted MEFs were then co-cultured with C2C12 myoblasts and stimulated to undergo differentiation. Results showed that iNOS silencing led to a significant reduction in the average number of nuclei per fiber as compared with control siRNA conditions (Fig. 7C). Con-
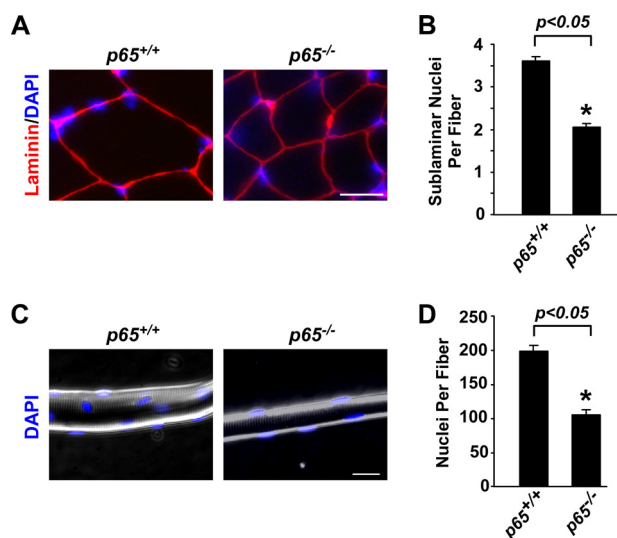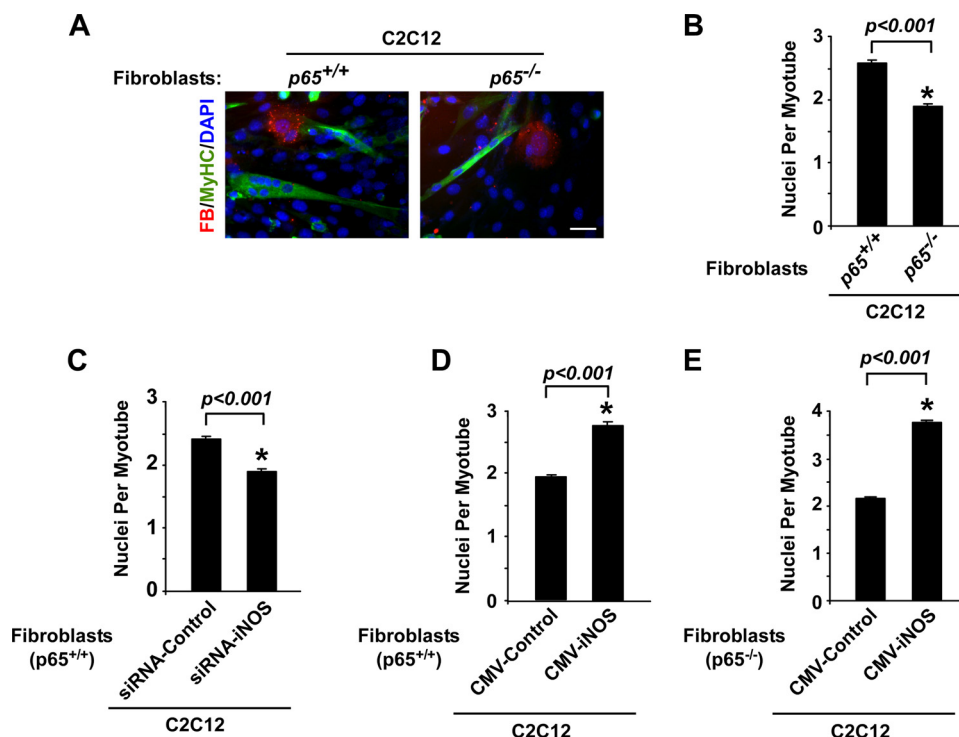

FIGURE 7. iNOS expression regulates myoblast fusion. *A* and *B*, $p65^{+/+}$ and $p65^{-/-}$ fibroblasts (*FB; red*) were stained with 20 μM Cell Tracker Orange CMTMR and co-cultured for 24 h with C2C12 myoblasts. After 24 h of co-culturing, cells were switched to differentiation media, and myogenesis proceeded for 3 days after which cells were fixed and stained with MyHC (*green*) and DAPI (*blue*). Nuclei per myotube numbers were determined as described under "Experimental Procedures." *Scale bar* = 40 μm. *C* and *D*, a similar analysis as described above was performed using wild type MEFs transfected with control or iNOS siRNA oligomers (*C*) or with control or iNOS cytomegalovirus expression plasmids (*D*). *E*, a similar analysis as described in *A* was performed using $p65^{-/-}$ MEFs transfected with control or iNOS cytomegalovirus expression plasmids.
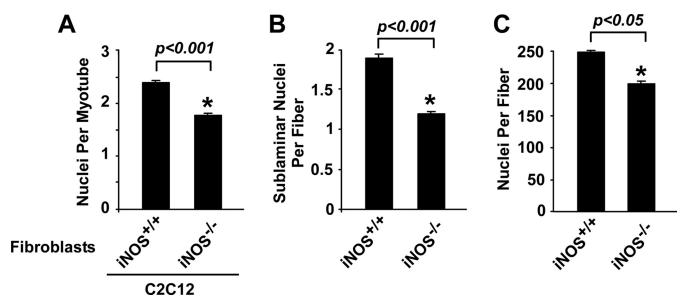
FIGURE 8. **Loss of iNOS expression inhibits myoblast fusion.** *A*, primary *iNOS*$^{+/+}$ and *iNOS*$^{-/-}$ fibroblasts were stained with 20 μM Cell Tracker Orange CMTMR and co-cultured for 24 h with C2C12 myoblasts. Differentiation was allowed to proceed for 3 days after which cells were fixed and stained with MyHC and DAPI and subsequently scored for nuclei per myotube. *B*, TA muscles from 4-week-old *iNOS*$^{+/+}$ and *iNOS*$^{-/-}$ mice (*n* = 3) were sectioned and stained with laminin and DAPI. Sublaminar nuclei per fiber counts were determined by fluorescent microscopy. *C*, single fibers isolated from the gastrocnemius muscles of 4-week-old *iNOS*$^{+/+}$ and *iNOS*$^{-/-}$ mice were stained with DAPI and analyzed by fluorescent and phase contrast microscopy to quantitate nuclei per fiber. Quantitation for *A–C* was performed as described under "Experimental Procedures."

versely, exogenous expression of iNOS in wild type (supplemental Fig. 5, *C* and *D*) or *p65*$^{-/-}$ MEFs, whose endogenous expression levels of iNOS are mostly absent (supplemental Fig. 5, *E* and *F*), enhanced myotube nucleation in this co-culture system (Fig. 7, *D* and *E*). These data suggest that iNOS expression emanating from the fibroblast compartment regulates myogenesis by modulating myoblast fusion.

Finally, to confirm the relevance of iNOS function with regard to myoblast fusion during postnatal muscle growth, we purified muscle fibroblasts from P8 *iNOS*$^{+/+}$ and *iNOS*$^{-/-}$ mice and performed a similar C2C12 co-culture analysis as described above. Consistent with our findings, we observed that the average number of nuclei per myotube was decreased by 26% in *iNOS*$^{-/-}$ co-cultures (Fig. 8*A*). We also observed a 50% reduction in the number of myotubes containing 4 or more nuclei in *iNOS*$^{-/-}$ *versus* *iNOS*$^{+/+}$ co-cultures (data not shown). We next quantitated sublaminar myonuclei from the muscles of 4-week-old *iNOS*$^{+/+}$ and *iNOS*$^{-/-}$ mice. In agreement with *in vitro* co-culture results, a significant reduction in the average number of sublaminar nuclei was observed in iNOS-deficient muscles (Fig. 8*B*). Likewise, nuclei numbers were also lower when scoring was performed on individual muscle fibers from *iNOS*$^{-/-}$ compared with *iNOS*$^{+/+}$ mice (Fig. 8*C*). However, unlike the deletion or inhibition of NF-κB shown in Fig. 1, global loss of iNOS expression did not cause an increase in myofiber number (supplemental Fig. 6), strongly arguing that iNOS function in postnatal muscle growth is restricted to modulating myoblast fusion. These data further support the notion that this function of iNOS in muscle stromal fibroblasts is firmly under NF-κB control.

DISCUSSION

Recent findings have illustrated the ability of NF-κB to function as an inhibitor of skeletal myogenesis (19, 24, 25). The purpose of this study was to characterize the role of NF-κB during early postnatal muscle development. During this investigation we determined that NF-κB activity is relatively high during the first 2 weeks of postnatal development, and inhibition of this activity resulted in both an increase in total muscle

fibers as well as an enhancement in the expression of early and late myogenic genes. These data underscore the ability of NF-κB to function as a potent regulator of skeletal muscle development during this early stage of postnatal growth. To determine how NF-κB is involved in this developmental process, we examined which cells within the maturing muscle contain active NF-κB. This led us to uncover some novel findings with respect to the cellular compartmentalization of NF-κB and its associated functions.

Results obtained from EGFP reporter mice revealed that the high levels of NF-κB present in skeletal muscle at birth and throughout the first days of neonatal development derived from myofibers. Our genetic analysis showing that conditional deletion of IKKβ in myofibers leads to an increase in total fiber number indicates that myofiber-specific activation of NF-κB at birth and shortly afterward serves to ensure that myogenesis is efficiently repressed. Presumably, this myogenic inhibitory activity is necessary to allow myoblasts to migrate and fuse to the surrounding fibers rather than initiate another round of myogenic differentiation, which may be disadvantageous for skeletal muscle hypertrophy. How NF-κB signaling in myofibers functions to repress myogenesis is not known but may be related to a secreted factor under NF-κB transcriptional control. Interestingly, in dystrophic myofibers of *mdx* mice that contain constitutively active NF-κB, deletion of IKKβ also leads to increases in new fiber formation (24). One factor associated with this regulation is TNFα, an inflammatory cytokine that acts as a potent inhibitor of myogenesis (19, 20). In an independent on-going study, we have found that TNFα is capable of suppressing the synthesis of the Notch-1 receptor, which under normal conditions is recognized as a critical regulator of satellite cell activation in response to muscle injury (37).[3] NF-κB-dependent production of TNFα from dystrophic myofibers that function to block Notch signaling in satellite cells might, therefore, be a mechanism by which NF-κB limits the regenerative capacity of skeletal muscle lacking dystrophin. With respect to our current findings, we considered the possibility that NF-κB activation in neonatal myofibers might repress myogenesis by a similar mechanism involving TNFα. However, to this point we have been unable to find differences in total fiber number when comparing muscle sections from *TNFα*$^{+/+}$ and *TNFα*$^{-/-}$ newborn mice.[4] Although it remains possible that the absence of a muscle phenotype in the *TNFα*$^{-/-}$ neonates is due to a compensating factor, at least at this level of investigation, our results suggest that the manner in which NF-κB functions to repress muscle differentiation in neonatal mice may be distinct from the mechanism utilized to limit myogenesis in states of chronic muscle injury.

An additional revealing finding from our study was the switch in NF-κB activity that occurred from myofibers at birth to stromal fibroblasts shortly after the first week of postnatal development. Further characterization of these fibroblasts showed that they provide a rich source of iNOS expression under the control of NF-κB. Past studies have shown that stimulated expression of iNOS modulates the production of NO by

---

converting L-arginine to citrulline (51, 52), which in turn contributes to myoblast fusion *in vitro* (48, 49, 53). In addition, treatment of differentiating primary muscle progenitor cells with exogenous NO yields an increase in fusion capacity when NO is administered within the first 24 h of differentiation (54). It has been demonstrated *in vitro* that differentiating primary myoblasts up-regulate iNOS expression to facilitate fusion and terminal differentiation (53). However, unknown to this point are the cells that contribute *in vivo* to NO production for myoblast fusion. Our findings highlight for the first time the importance of stromal fibroblasts in developing postnatal skeletal muscle by showing that such cells provide a source of NO under the regulation of NF-κB, which presumably is critical for coordinating myoblast fusion during the hypertrophic phase of maturing skeletal muscle.

Classical NF-κB activity was recently identified by genetic means to act as an inhibitor of myogenesis either *in vitro* or in adult mouse muscles in response to acute or chronic injury (24, 25). In contrast, alternative NF-κB signaling is regulated by IKKα homodimers and promotes p100 to p52 processing. The pathway itself is thought to be dispensable for myogenesis but required for mitochondrial biogenesis during differentiation and the formation of energetically competent myofibers (25). Our findings support that high NF-κB activity present in muscles of newborn mice derives from the classical pathway. Likewise, the activities associated with stromal fibroblasts and iNOS synthesis are dependent on p65, one of the classical subunits of NF-κB. Whether alternative signaling is also involved during this maturation stage of postnatal muscle development is not known. However, immunoblotting for p100 revealed a clear increase in p52 expression 2 weeks after birth (supplemental Fig. 7). This is in contrast to classical NF-κB signaling whose activity declined over a similar two-week period. Intriguingly, this same inverse relationship between classical and alternative signaling occurs during differentiation of C2C12 myoblasts (25). The significance of this increase in alternative signaling observed during postnatal muscle growth remains to be explored.

Collectively, our findings illustrate important roles of NF-κB in different cell types during early skeletal muscle development. Although NF-κB has been found to associate with myofibers and muscle residing macrophages (24), this is the first report describing its localization to muscle fibroblasts. In neonatal conditions, we find that fibroblast-specific activation of NF-κB stimulates iNOS expression and promotes myoblast fusion and muscle hypertrophy. This activity is distinct from NF-κB activity derived from myofibers, which acts instead to repress myogenesis. Future work will decipher whether such compartmentalized functions of NF-κB are recapitulated in adult skeletal muscle undergoing growth and regeneration.

REFERENCES

1. Baeuerle, P. A., and Baltimore, D. (1996) *Cell* **87,** 13–20
2. Baldwin, A. S., Jr. (1996) *Annu. Rev. Immunol.* **14,** 649–683
3. Verma, I. M., Stevenson, J. K., Schwarz, E. M., Van Antwerp, D., and Miyamoto, S. (1995) *Genes Dev.* **9,** 2723–2735
4. Hayden, M. S., and Ghosh, S. (2004) *Genes Dev.* **18,** 2195–2224
5. Li, Z., and Nabel, G. J. (1997) *Mol. Cell. Biol.* **17,** 6184–6190
6. Chen, F. E., and Ghosh, G. (1999) *Oncogene* **18,** 6845–6852
7. Baeuerle, P. A., and Henkel, T. (1994) *Annu. Rev. Immunol.* **12,** 141–179
8. Bonizzi, G., and Karin, M. (2004) *Trends Immunol.* **25,** 280–288
9. Ghosh, S., and Karin, M. (2002) *Cell* **109,** S81–S96
10. Hu, Y., Baud, V., Oga, T., Kim, K. I., Yoshida, K., and Karin, M. (2001) *Nature* **410,** 710–714
11. Ruocco, M. G., Maeda, S., Park, J. M., Lawrence, T., Hsu, L. C., Cao, Y., Schett, G., Wagner, E. F., and Karin, M. (2005) *J. Exp. Med.* **201,** 1677–1687
12. Guttridge, D. C., Albanese, C., Reuther, J. Y., Pestell, R. G., and Baldwin, A. S., Jr. (1999) *Mol. Cell. Biol.* **19,** 5785–5799
13. Buckingham, M. (2001) *Curr. Opin. Genet. Dev.* **11,** 440–448
14. Williams, B. A., and Ordahl, C. P. (1994) *Development* **120,** 785–796
15. Naya, F. J., and Olson, E. (1999) *Curr. Opin. Cell Biol.* **11,** 683–688
16. Pownall, M. E., Gustafsson, M. K., and Emerson, C. P., Jr. (2002) *Annu. Rev. Cell Dev. Biol.* **18,** 747–783
17. Sabourin, L. A., and Rudnicki, M. A. (2000) *Clin. Genet.* **57,** 16–25
18. Lehtinen, S. K., Rahkila, P., Helenius, M., Korhonen, P., and Salminen, A. (1996) *Biochem. Biophys. Res. Commun.* **229,** 36–43
19. Guttridge, D. C., Mayo, M. W., Madrid, L. V., Wang, C. Y., and Baldwin, A. S., Jr. (2000) *Science* **289,** 2363–2366
20. Langen, R. C., Van Der Velden, J. L., Schols, A. M., Kelders, M. C., Wouters, E. F., and Janssen-Heininger, Y. M. (2004) *FASEB J.* **18,** 227–237
21. Caretti, G., Di Padova, M., Micales, B., Lyons, G. E., and Sartorelli, V. (2004) *Genes Dev.* **18,** 2627–2638
22. Wang, H., Garzon, R., Sun, H., Ladner, K. J., Singh, R., Dahlman, J., Cheng, A., Hall, B. M., Qualman, S. J., Chandler, D. S., Croce, C. M., and Guttridge, D. C. (2008) *Cancer Cell* **14,** 369–381
23. Wang, H., Hertlein, E., Bakkar, N., Sun, H., Acharyya, S., Wang, J., Carathers, M., Davuluri, R., and Guttridge, D. C. (2007) *Mol. Cell. Biol.* **27,** 4374–4387
24. Acharyya, S., Villalta, S. A., Bakkar, N., Bupha-Intr, T., Janssen, P. M., Carathers, M., Li, Z. W., Beg, A. A., Ghosh, S., Sahenk, Z., Weinstein, M., Gardner, K. L., Rafael-Fortney, J. A., Karin, M., Tidball, J. G., Baldwin, A. S., and Guttridge, D. C. (2007) *J. Clin. Invest.* **117,** 889–901
25. Bakkar, N., Wang, J., Ladner, K. J., Wang, H., Dahlman, J. M., Carathers, M., Acharyya, S., Rudnicki, M. A., Hollenbach, A. D., and Guttridge, D. C. (2008) *J. Cell Biol.* **180,** 787–802
26. Mourkioti, F., Kratsios, P., Luedde, T., Song, Y. H., Delafontaine, P., Adami, R., Parente, V., Bottinelli, R., Pasparakis, M., and Rosenthal, N. (2006) *J. Clin. Invest.* **116,** 2945–2954
27. Doi, T. S., Marino, M. W., Takahashi, T., Yoshida, T., Sakakura, T., Old, L. J., and Obata, Y. (1999) *Proc. Natl. Acad. Sci. U.S.A.* **96,** 2994–2999
28. Beg, A. A., Sha, W. C., Bronson, R. T., Ghosh, S., and Baltimore, D. (1995) *Nature* **376,** 167–170
29. Karrasch, T., Kim, J. S., Muhlbauer, M., Magness, S. T., and Jobin, C. (2007) *J. Immunol.* **178,** 6522–6532
30. Li, Z. W., Omori, S. A., Labuda, T., Karin, M., and Rickert, R. C. (2003) *J. Immunol.* **170,** 4630–4637
31. Bilic-Curcic, I., Kronenberg, M., Jiang, X., Bellizzi, J., Mina, M., Marijanovic, I., Gardiner, E. M., and Rowe, D. W. (2005) *Genesis* **43,** 87–98
32. Rando, T. A., and Blau, H. M. (1994) *J. Cell Biol.* **125,** 1275–1287
33. Cheshire, J. L., and Baldwin, A. S., Jr. (1997) *Mol. Cell. Biol.* **17,** 6746–6754
34. Shefer, G., and Yablonka-Reuveni, Z. (2005) *Methods Mol. Biol.* **290,** 281–304
35. Acharyya, S., Ladner, K. J., Nelsen, L. L., Damrauer, J., Reiser, P. J., Swoap, S., and Guttridge, D. C. (2004) *J. Clin. Invest.* **114,** 370–378
36. Artaza, J. N., Bhasin, S., Magee, T. R., Reisz-Porszasz, S., Shen, R., Groome, N. P., Meerasahib, M. F., Fareez, M. M., and Gonzalez-Cadavid, N. F. (2005) *Endocrinology* **146,** 3547–3557

37. Conboy, I. M., and Rando, T. A. (2002) *Dev. Cell* **3,** 397–409
38. Delfini, M. C., Hirsinger, E., Pourquié, O., and Duprez, D. (2000) *Development* **127,** 5213–5224
39. Karin, M. (1999) *J. Biol. Chem.* **274,** 27339–27342
40. Mercurio, F., Zhu, H., Murray, B. W., Shevchenko, A., Bennett, B. L., Li, J., Young, D. B., Barbosa, M., Mann, M., Manning, A., and Rao, A. (1997) *Science* **278,** 860–866
41. Sakurai, H., Suzuki, S., Kawasaki, N., Nakano, H., Okazaki, T., Chino, A., Doi, T., and Saiki, I. (2003) *J. Biol. Chem.* **278,** 36916–36923
42. Yang, F., Tang, E., Guan, K., and Wang, C. Y. (2003) *J. Immunol.* **170,** 5630–5635
43. Faigle, W., Colucci-Guyon, E., Louvard, D., Amigorena, S., and Galli, T. (2000) *Mol. Biol. Cell* **11,** 3485–3494
44. Floss, T., Arnold, H. H., and Braun, T. (1997) *Genes Dev.* **11,** 2040–2051
45. Johnson, S. E., and Allen, R. E. (1990) *Exp. Cell Res.* **187,** 250–254
46. Soulet, L., Chevet, E., Lemaitre, G., Blanquaert, F., Meddahi, A., and Barritault, D. (1994) *Mol. Reprod. Dev.* **39,** 49–55
47. Anderson, J. E. (2000) *Mol. Biol. Cell* **11,** 1859–1874
48. Lee, K. H., Baek, M. Y., Moon, K. Y., Song, W. K., Chung, C. H., Ha, D. B., and Kang, M. S. (1994) *J. Biol. Chem.* **269,** 14371–14374
49. Long, J. H., Lira, V. A., Soltow, Q. A., Betters, J. L., Sellman, J. E., and Criswell, D. S. (2006) *J. Muscle Res. Cell Motil.* **27,** 577–584
50. Wozniak, A. C., and Anderson, J. E. (2007) *Dev. Dyn.* **236,** 240–250
51. Nathan, C. (1992) *FASEB J.* **6,** 3051–3064
52. Nathan, C., and Xie, Q. W. (1994) *Cell* **78,** 915–918
53. Lee, K. H., Kim, D. G., Shin, N. Y., Song, W. K., Kwon, H., Chung, C. H., and Kang, M. S. (1997) *Biochem. J.* **324,** 237–242
54. Pisconti, A., Brunelli, S., Di Padova, M., De Palma, C., Deponti, D., Baesso, S., Sartorelli, V., Cossu, G., and Clementi, E. (2006) *J. Cell Biol.* **172,** 233–244